Received: 5 October 2018 | Revised: 6 February 2019 | Accepted: 1 March 2019

DOI: 10.1002/hbm.24570

WILEY

RESEARCH ARTICLE

The situation or the person? Individual and task-evoked differences in BOLD activity

Taylor Bolt[1] | Jason S. Nomi[2] | Sierra A. Bainter[2] | Michael W. Cole[3] | Lucina Q. Uddin[2,4]

[1]Gallup, Data Science Division, Washington, DC

[2]Department of Psychology, University of Miami, Coral Gables, Florida

[3]Center for Molecular and Behavioral Neuroscience, Rutgers University, Newark, New Jersey, USA

[4]Neuroscience Program, University of Miami Miller School of Medicine, Miami, Florida

Correspondence
Taylor Bolt, Department of Psychology, University of Miami, P.O. Box 248185, Coral Gables, Florida 33124, USA.
Email: tsb46@miami.edu

Abstract

Investigations of between-person variability are enjoying a recent resurgence in functional magnetic resonance imaging (fMRI) research. Several recent studies have found persistent between-person differences in blood-oxygenated-level dependent (BOLD) activation patterns and resting-state functional connectivity. Conflicting findings have been reported regarding the extent to which (a) between-person or (b) within-person cognitive state differences explain differences in BOLD activation patterns. These discrepancies may arise due to statistical analysis choices, parcellation resolution, and limited sampling of task-fMRI datasets. We attempt to address these issues in a large-scale analysis of several task-fMRI paradigms. Using a novel application of multivariate distance matrix regression, we examine between-person and task-condition variability estimates across varying levels of "resolution", from a coarse region-of-interest level to the vertex-level, and across different distance metrics. These analyses revealed that under most circumstances, differences in task conditions explained a greater amount of variance in activation map differences than between-person differences. However, this finding was reversed when comparing activation maps at a "high-resolution" vertex level. More generally, we observed that when moving from "low" to "high" resolutions, the variance explained by between-person differences increased while variance explained by task conditions decreased. We further analyzed the relationships among subject-level activation maps across all task-conditions using an unsupervised clustering approach and identified a superordinate task structure. This structure went beyond conventional task labels and highlighted those experimental manipulations across task conditions that produce contrasting versus similar whole-brain activation patterns. Overall, these analyses suggest that the question of the subject- versus task-effects on BOLD activation patterns is nontrivial, and depends on the comparison "resolution," choice of distance metric, and the coding of task-conditions.

KEYWORDS

individual differences, intersubject variability, task-fMRI

1 | INTRODUCTION

Conventional group-level analyses in task-based functional magnetic resonance imaging (task-fMRI) disregard between-subject variability as noise, with the strong assumption that spatial and temporal activity is similar across subjects. Recent cognitive neuroscience research has challenged this assumption (Seghier & Price, 2018). Several recent studies have shown that between-person variability is a ubiquitous feature of blood-oxygenated-level dependent (BOLD) activation patterns and resting-state functional connectivity (Finn et al., 2015; Gordon et al., 2017; Gratton et al., 2018; Miller, Donovan, Bennett, Aminoff, & Mayer, 2012; Rosenberg, Finn, Scheinost, Constable, & Chun, 2017). In fact, several earlier studies by Miller et al. (2002, 2009, 2012) found that between-person differences in whole-brain BOLD activation patterns persist across differences in task conditions. Specifically, they found that whole-brain activation patterns were more similar across conditions within the *same subject* than activation patterns across subjects in the *same condition*. In contrast, a recent study of task-related changes in functional connectivity and whole-brain activation by Gratton et al. (2018) found that whole-brain activation

patterns are driven more by differences in task conditions than by persistent individual differences. Thus, the relative contribution of between-person versus cognitive state changes has yet to be clarified. We identify three potential factors contributing to the inconsistency in findings: (a) Estimation of between-subject and task-condition variability, (b) the spatial resolution at which activation maps are compared, and (c) the choice of task-fMRI paradigms.

Previous analyses of between-person differences in whole-brain activation patterns (Miller et al., 2009, 2012; Gratton et al., 2018) relied on comparisons of the *average* pair-wise correlation of whole-brain activation maps across subjects versus task conditions. As such, these previous analyses do not provide estimates of the variance in whole-brain activation map *differences* explained by either between-person or task condition differences. To estimate the unique variance in whole-brain activation pattern differences explained by subject and experimental factors, we use a regression-based approach for distance matrices, known as multivariate distance matrix regression (MDMR; Shehzad et al., 2014; Zapala & Schork, 2006). As a simple extension of the multiple regression framework, MDMR on whole-brain activation pattern distance matrices provides explained variance estimates for both between-person and task-condition factors. To the best of our knowledge, this is the first application of MDMR to understand between-person and task condition variability in BOLD activation patterns. We applied MDMR to a large set of task-fMRI paradigms to examine between-person variability in whole-brain activation pattern across task-paradigms.

While some have compared whole-brain activation maps at a voxel-level (Miller et al., 2009), others have compared whole-brain activation maps at a coarser region-of-interest (ROI) level (Gratton et al., 2018). The brain is hierarchically organized, and even at the level of current whole-brain BOLD fMRI imaging (~2 mm), there is no "optimal" parcellation resolution (e.g., 300 vs. 600 ROIs) (Eickhoff, Constable, & Yeo, 2018; Schaefer et al., 2017). However, the resolution at which subject whole-brain activation maps are compared is likely to have a moderate, if not dramatic, effect on estimates of between-person and task-condition variability. For example, regional BOLD changes due to stimulus presentation may exhibit the same coarse spatial pattern across subjects, yet small spatial scale changes in this overall pattern may be present. In this case, a coarse ROI parcellation (e.g., 200 ROIs) may underestimate the degree of between-person variability, as compared with task-conditions. To understand the effect of "resolution" on between-person variability estimates, we conducted an MDMR analysis on a range of "resolutions" using a recently developed multi-resolution parcellation scheme (Schaefer et al., 2017).

A third factor contributing to the aforementioned inconsistent findings may be the choice of task paradigm. Different paradigms involve different task demands and sensory modalities. In addition, many task paradigms afford more or less variability in the strategies utilized. For example, a variety of different encoding strategies can be utilized when performing an episodic-memory retrieval task (Bernstein, Beig, Siegenthaler, & Grady, 2002; Miller et al., 2012). Importantly, different strategies applied to the same task are associated with different whole-brain activation patterns (Delgado, Gillis, & Phelps, 2008; Fink, Marshall, Weiss, Toni, & Zilles, 2002; Iaria, Petrides, Dagher, Pike, & Bohbot, 2003; Miller et al., 2009, 2012). Therefore, the level of inter-subject variability in whole-brain activation patterns may be dependent on the type of task paradigm used. One might predict that "lower-order" tasks, such as simple sensory-motor tasks afford less inter-subject variability in strategy than "higher-order" tasks, such as working-memory or social cognition tasks, and thus, less inter-subject variability in whole-brain activation patterns.

Accordingly, the amount of variance explained by task conditions would depend on how these conditions are categorized. Two task conditions eliciting the same neural mechanisms will presumably yield the same whole-brain pattern of BOLD activity, and thus, the distinction between these two task conditions will explain little or no variability in whole-brain BOLD activation patterns. Though it is quite common to assume two task conditions with different stimuli and task demands elicit different whole-brain BOLD activation patterns, this is not always the case. For example, it has been shown that activation patterns produced by "task-switching" paradigms are statistically indistinguishable from those produced by "working-memory," "response-inhibition," and "response-selection" paradigms (Lenartowicz, Kalar, Congdon, & Poldrack, 2010). On the other hand, two task conditions eliciting widely different neural mechanisms will explain a greater amount of variability in whole-brain BOLD activation patterns. These issues related to the recent discussion of a brain-based "cognitive" ontology or taxonomy (Bolt, Nomi, Yeo, & Uddin, 2017; Poldrack & Yarkoni, 2016), using task-fMRI BOLD activation patterns to delineate categories of cognitive processes or mechanisms. In relation to the above discussion, the variance explained by task conditions will depend on how these task conditions are *coded*, meaning which task conditions we distinguish from each other. To examine interrelationships among differently coded task conditions, we use a graph-based clustering approach to identify clusters of similar whole-brain activation maps across all task conditions.

To assess the contribution of these factors to between-person and task condition variability estimates, we analyze task-fMRI data provided by the Human Connectome Project (HCP; Barch et al., 2013). To summarize, the primary goals of this study are (a) to use a novel MDMR analytic approach to simultaneously estimate the unique variance in whole-brain BOLD activation map differences explained by between-person and task condition variability, (b) to assess the influence of cortical parcellation "resolution" on between-person variability estimates, and (c) to assess the choice and coding of task paradigm on between-person variability estimates.

2 | MATERIALS AND METHODS

2.1 | Task descriptions

Surface-based activation maps were collected from 416 unrelated, healthy subjects provided by the HCP (Van Essen et al., 2013) as they performed seven tasks: Emotion, gambling, language, motor, relational, social, and working memory. A brief description of each HCP task is presented here, but for more details see Barch et al. (2013). The working-memory task was an N-back task with eight condition types of 0-back and 2-back conditions with faces, places, tools, and

body parts presented as stimuli. The gambling task was a card guessing game, which involved guessing the number on a mystery card to win or lose money in two different conditions: "mostly win" or "mostly lose" outcome conditions. In the motor task, there were six condition types where subjects were directed to perform particular motor movements from the fingers, toes, or tongue in response to visual cues. The language task was a story-comprehension task with interleaved blocks of two condition types: Brief auditory stories and simple arithmetic problems (e.g., "fourteen plus twelve."). The social task was a "theory of mind" task where participants are presented with short video clips of two condition types: Interacting or randomly moving shapes. In the relational task, subjects are presented with pairs of objects and told to distinguish them on either subject-specified dimensions in one condition or experimenter-specified dimensions in the other condition. In the emotion task, participants were told to match either emotionally expressive faces (e.g., angry or fearful) in one condition or shapes in the other condition. In total, each subject completed 24 task conditions across the seven tasks.

2.2 | Task-fMRI preprocessing and analysis

A detailed description of the HCP structural and functional minimal-preprocessing pipeline is provided in Glasser et al. (2013). We briefly describe the surface-based functional preprocessing and analysis pipeline relevant to the question of inter-subject variability: (a) Subject's volume scans are mapped to CIFTI gray-ordinates standard space (32k Conte69 mesh) using an advanced "areal-feature-based" multi-modal registration algorithm (MSMAll; features used included myelin maps, resting-state networks, and resting state topographic maps), (b) 2 mm FWHM surface-based smoothing using a geodesic Gaussian algorithm, (c) 2 mm subcortical parcel-constrained smoothing (only the cortical surface vertices were used in subsequent analyses), and (d) conversion to CIFTI dense time series format for further processing. Subsequent preprocessing included an extra surface-based smoothing using a geodesic Gaussian algorithm with 4 mm FWHM (no further smoothing was conducted). Computation of whole-brain activation maps for each subject was computed using a standard general linear model (GLM) analysis using FSL's FMRIB's Improved Linear Model (FILM) with autocorrelation correction (Woolrich, Ripley, Brady, & Smith, 2001). Task condition regressors were constructed by convolution with a canonical hemodynamic response function (HRF; Glover, 1999). Temporal derivatives of each convolved regressor were included in the GLM to account for timing differences, but estimates for these terms were not used for the analysis. The standardized beta estimates (z-statistics) were used as BOLD "activation" estimates for each vertex and used in further analyses.

2.3 | Construction of whole-brain activation map distance matrices

Whole-brain activation map distance matrices were constructed at the vertex-level, and across a range of resolution sizes at a ROI level (N = 100, 200, 400, 600, and 800; higher number of ROIs corresponds to a more fine-grained parcellation) using the whole-cortex Schaefer parcellation (Schaefer et al., 2017). Activation estimates for each ROI were calculated as the mean standard beta estimate for all vertices contained within the ROI. As whole-brain *cortical* activation patterns were of interest, noncortical vertices were excluded from the computation of the distance matrix. The "distance" between two whole-brain activation maps represents the dissimilarity in activation estimates (estimated from the GLM described above) of all vertices or ROIs between each map. Note, the activation estimates for all vertices or ROIs were *not* thresholded before the distance computation, meaning the activation estimates of all vertices or ROIs contributed to the distance computation. The whole-brain activation map distance matrix was constructed by computing both the City block (L1-norm) and Euclidean (L2-norm) distance metrics between all pairs of whole-brain activation maps across all subjects. Vertex- and ROI-values of each activation maps were z-score standardized before computation of distance to remove arbitrary mean and scaling differences. Pearson correlation and cosine distance, both equivalent (up to a constant factor) to *squared* Euclidean distance on z-scored data (Berthold & Höppner, 2016), were attempted but resulted in a singular distance matrix with negative sums of squares residual estimates in the MDMR analysis ($R^2 > 1$). However, the relative difference between the task condition versus subject estimates was similar for the correlation/cosine distance and Euclidean distances. The whole-brain activation map distance matrix is constructed by computing the distance (City block or Euclidean) between all subject's task-condition activation maps (N = 24 task-conditions). The resultant 9,984 (416 subjects × 24 task-conditions) by 9,984 task-activation map distance matrix was then input to the MDMR analysis. An illustration of this process on a hypothetical task-fMRI dataset of two subjects and two tasks is presented in Figure 1.

2.4 | Multivariate distance matrix regression

2.4.1 | Omnibus analysis

MDMR was used to quantify the variability in whole-brain activation map dissimilarity explained by between-person or task condition differences. We ran two MDMR models with two types of task dummy-codes: One in which only the task paradigm is coded (ignoring separate conditions within each task paradigm), and one in which all conditions of each task paradigm are coded. The statistic of interest was the explained variance (R^2) estimates for the subject and task dummy-coded predictors. Comparison of the explained variance estimates between the task paradigm and task condition dummy-coded models provide an estimate of how much explained variance is added to the model when conditions within each task paradigm are added to the model. These analyses were conducted on the whole-brain activation map distance matrices constructed from both the vertex-level data and Schaefer ROI-parcellations. The "statistical significance" of the mean difference between task condition and between-person R^2 estimates was tested using bootstrapped confidence intervals (N = 100). In particular, clustered bootstrapping was used, where "subjects" (all 24 task-condition activation maps) were resampled with replacement, as opposed to individual task condition maps within subjects, to account for the nested structure of the data.

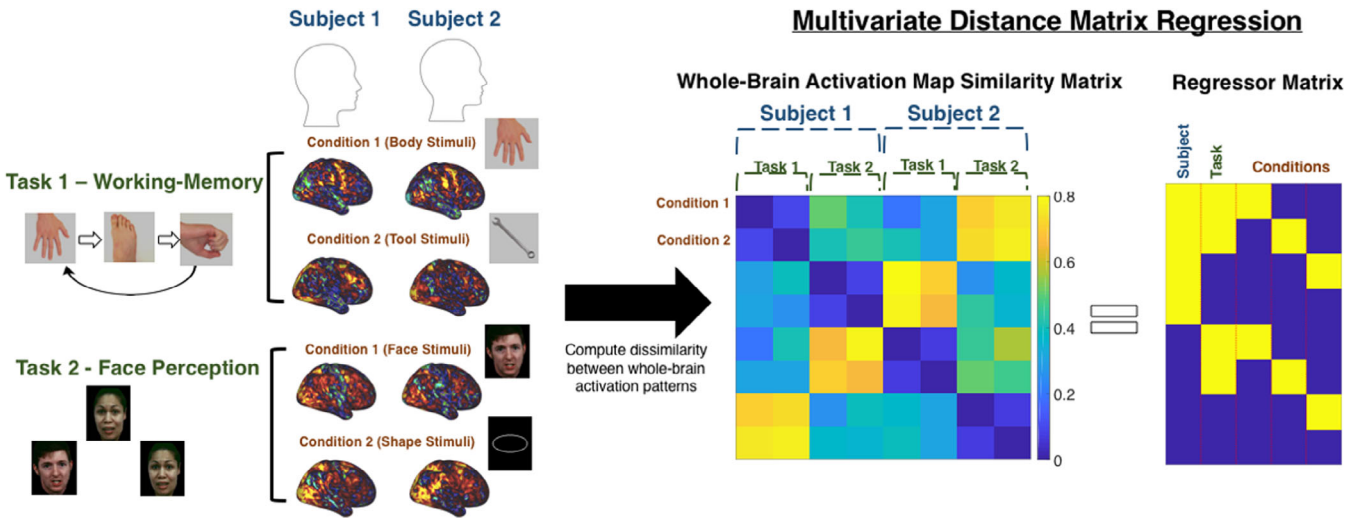

FIGURE 1 Example MDMR analysis of whole-brain activation patterns. An example MDMR analysis of two subjects performing two hypothetical tasks, a working-memory (N-back task) and a face perception task. For each task, there are two separate conditions: Body and tool stimuli for the working-memory task, and faces and shapes for the face perception task. Whole-brain activation patterns are computed for the two conditions of each task using the conventional GLM approach. To construct a distance matrix, dissimilarity estimates are computed between all pairs of whole-brain activation patterns, where higher values represent greater dissimilarity in whole-brain activation patterns. The whole-brain activation pattern dissimilarity matrix is then regressed on a matrix of predictors representing subject, task paradigm, and condition factors using MDMR [Color figure can be viewed at wileyonlinelibrary.com]

Statistical significance was declared if the 95% percentile between the two R^2 bootstrapped distributions did not overlap.

2.4.2 | Post hoc task-paradigm specific analysis

To assess the between-person variability *within* each task-paradigm separately, we ran a post hoc MDMR model for each task paradigm. For each MDMR model, subject- and task-conditions were separately dummy-coded into two sets of categorical predictors and regressed onto task paradigm distance matrices. For five out of seven tasks (excluding the motor: 5 conditions and WM task: 8 conditions), only one dummy-variable for task condition was needed for an active- versus control-condition contrast. As in the task-general MDMR analysis above, the statistic of interest was the explained variance (R^2) estimates for the subject and task condition dummy-coded predictors.

2.5 | Clustering analysis

To further explore the organization between whole-brain activation maps, we applied the *Louvain* modularity maximization graph-clustering algorithm (Blondel, Guillaume, Lambiotte, & Lefebvre, 2008) to a whole-brain activation map similarity matrix. The whole-brain activation similarity matrix was computed from the Pearson correlation similarity between each whole-brain activation map using the $N = 100$ resolution Schaefer parcellation, as this was found to be most responsive to task differences (see Section 3). However, we also demonstrate that the partition from this ROI-parcellation resolution was minimally different from the partitions using higher-resolutions or vertex-level data. Roughly, the objective of the graph-clustering algorithm (implemented in the Brain Connectivity Toolbox; Rubinov & Sporns, 2010) is to partition the whole-brain activation maps into communities that maximize the within-cluster similarity of whole-brain activation patterns. Negative weights (i.e., negative correlation coefficients) were set to contribute asymmetrically to the modularity objective function (Rubinov & Sporns, 2011). In addition, an iterative fine-tuning algorithm was used that recursively applied the *Louvain* algorithm until no further increases in the modularity objective function were achieved (Geerligs, Rubinov, Cam-CAN, & Henson, 2015). Because modularity-maximization algorithms suffer from a well-known resolution limit (Fortunato & Barthélemy, 2007), the modularity objective function is often modified with a resolution parameter (Betzel & Bassett, 2016; Geerligs et al., 2015) to control the resulting "resolution" of the clusters. To choose a value for this parameter, we searched across a range of resolution parameter values, and chose the values that produced the most consistent partitions across 50 runs of the algorithm, measured as the average adjusted Rand index (Traud, Kelsic, Mucha, & Porter, 2011) using code provided in the Network Community toolbox (http://commdetect.weebly.com/). All values for the parameter from 0.75 to 1.04 yielded perfect across-run consistency, with a drop-off in consistency thereafter (Supporting Information Figure S3). There is a "rebound" after this drop-off in the consistency parameter at the value of 1.13. Thus, we present two clustering solutions at the following values of the resolution parameter, 1.04 and 1.13, that present a "coarse" and "fine-grained" view of the relationships among activation maps, respectively.

The resulting clusters provide insight into what types of task conditions drive the greatest differences among whole-brain activation patterns, and how consistent these differences are across subjects. To interpret each cluster, we inspected the number of activation maps from each task condition in each cluster. The number of task condition activation maps in each cluster were visualized in a word cloud created using the *wordcloud* function in MATLAB. To visualize the activation patterns associated with each cluster, we computed the average (centroid) activation pattern by computing the mean for all vertices across cluster members.

3 | RESULTS

3.1 | MDMR results

The results of the MDMR analysis revealed that task condition differences explained a greater amount of variance (100 ROI/City block: $R^2_{\text{task-paradigm}} = 0.3404$, $R^2_{\text{task-condition}} = 0.467$) in whole-brain activation patterns than between-person differences (100 ROI/City block: $R^2_{\text{subject}} = 0.143$) for all resolutions of the Schaefer parcellation (Figure 2). Of note, all comparisons of R^2 values were statistically significant, as confirmed by zero overlap in their bootstrapped R^2 distributions (visually apparent from Figure 2). This was true for both the City block distance and Euclidean distance. However, this finding was reversed at the vertex-level with the City block distance: Between-person differences explained a greater amount of variance in whole-brain activation patterns than did task paradigm. One contributing factor for this reversal is the "resolution" at which distances are computed: As the resolution increases from the 100 ROI Schaefer parcellation to the vertex-level, the amount of variance explained by task condition decreases, while between-person differences increases. Another contributing factor to this reversal is the differential emphasis on large distances by the City block and Euclidean distance metrics. The Euclidean distance metric places greater weight on large distances given that the difference between each vertex or ROI is squared, which is not the case with the City block metric. Thus, large activation differences in ROIs or vertices between task paradigms are given greater weight in the total distance calculation with the Euclidean distance metric. Together, these factors may explain the reversal observed between the vertex and ROI-level resolutions for the City block distance metric.

3.2 | Task-specific post hoc MDMR results

To further analyze between-person versus task condition variability of whole-brain activation patterns, we applied the MDMR analysis separately for each task, modeling both conditions within each task and between-person differences. The results suggest that *within a task paradigm*, between-person differences explain a substantially greater amount of variance than task condition differences of that task paradigm (Figure 3). The size of this difference was dependent on task

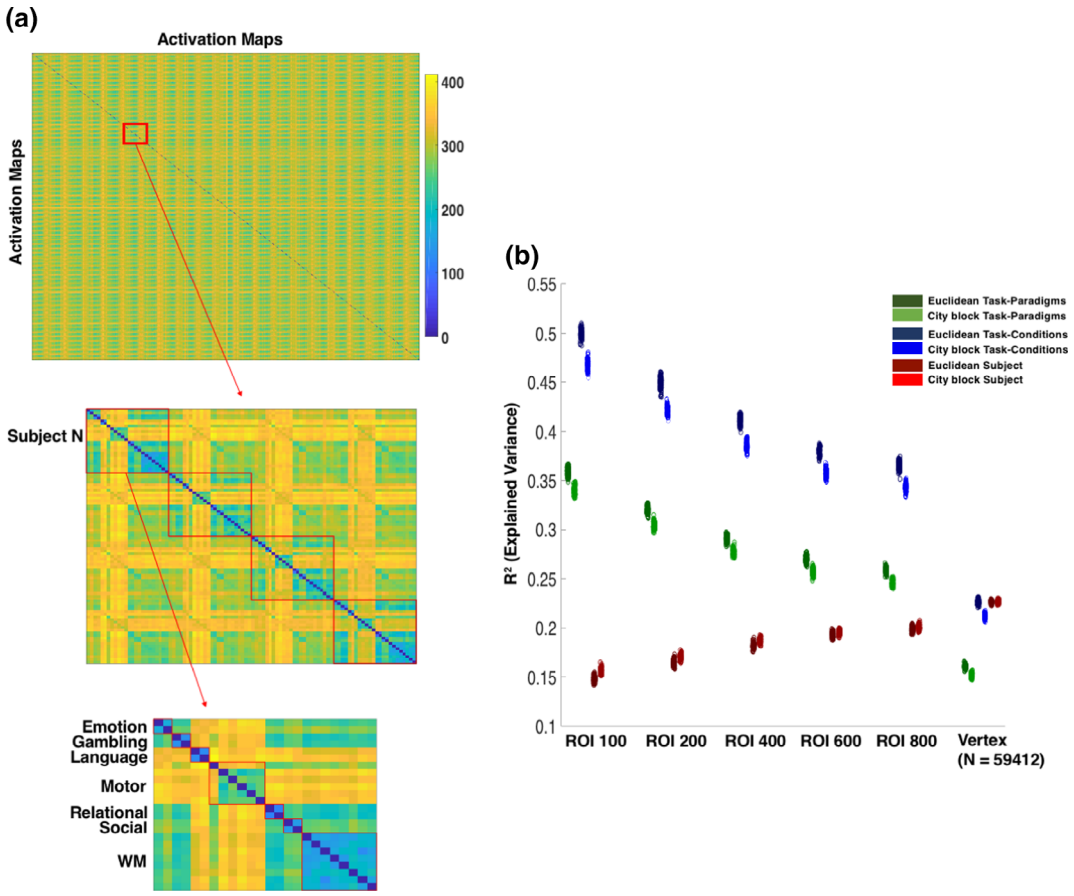

FIGURE 2 MDMR results. Whole-brain activation map Euclidean distance matrix and explained variance estimates across "resolution" sizes. (a) The whole-brain activation map Euclidean distance matrix presented in this figure was computed on vertex-level data. Each box from top to bottom presents a progressively more "fine-grained" view of the matrix, from the entire distance matrix (top), to a few subjects (middle), and a representative single subject (bottom). The pattern of distances within and across each task was similar across all resolutions and distance metrics (Euclidean and City block). (b) The graph in the right panel of the figure presents bootstrapped ($N = 100$) explained variance estimates for task paradigms (green; no conditions within the paradigm modeled), task-conditions (blue; conditions within each paradigm modeled), and subject (red). All bootstrapped explained variance estimates are presented as scatter plot points in a box-plot format to give a visualization of the variability in estimates across each bootstrapped sample. MDMR results on Euclidean and City block distance are presented in darker and brighter colors, respectively [Color figure can be viewed at wileyonlinelibrary.com]

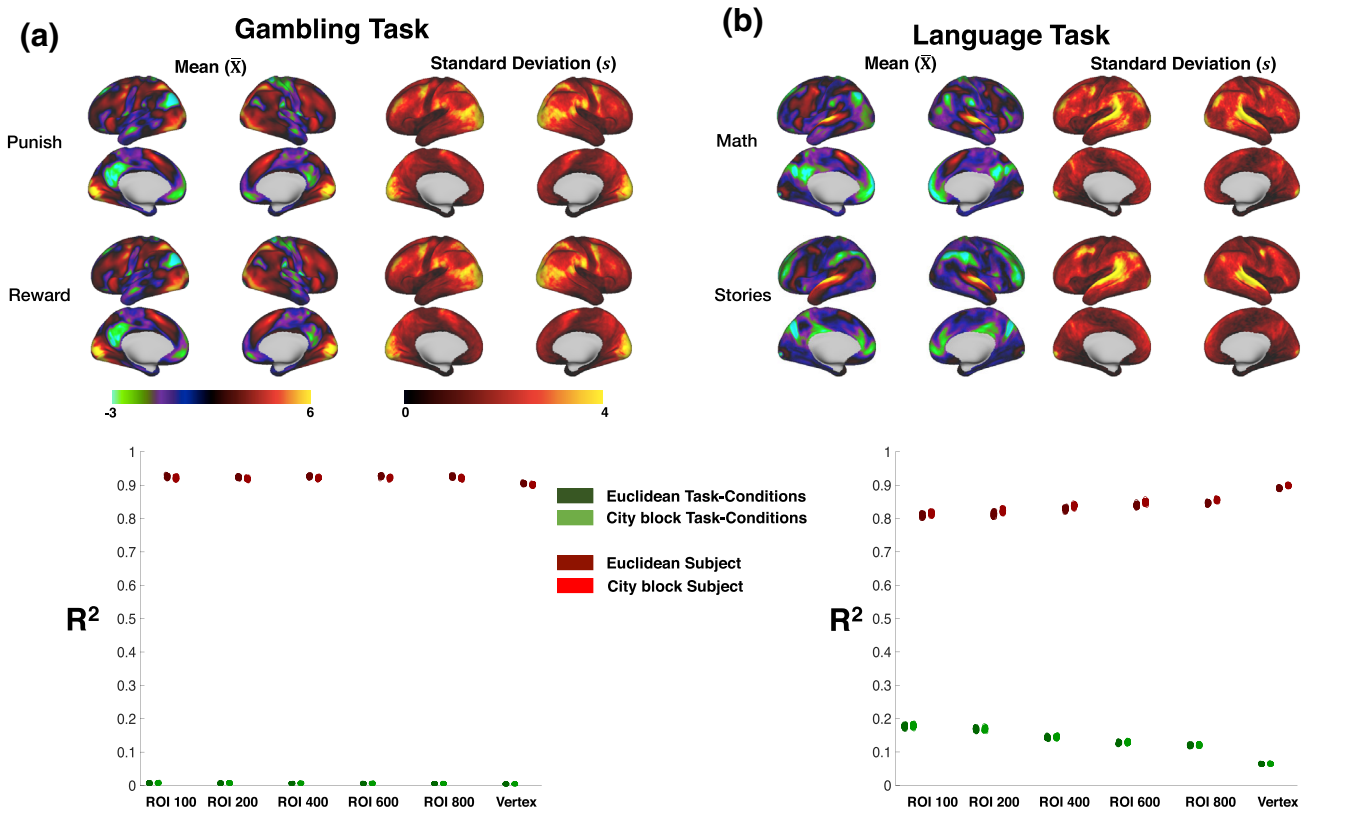

FIGURE 3 Task-specific MDMR analysis for gambling and language task. Explained variance estimates for task condition and subject factors, along with across-subject mean and *SD* maps for the (a) gambling and (b) language task. All task-paradigms are displayed in Supporting Information Figure S1. For each task paradigm, across-subject mean and *SD* maps for each task-condition are displayed side-by-side, and its associated explained variance estimate plots are presented below. Euclidean and city-block distance are presented in dark (dark red and dark green) and bright colors (bright red and bright green), respectively [Color figure can be viewed at wileyonlinelibrary.com]

paradigm. For example, in the Gambling task, the difference between the "punish" and "reward" conditions explained a minimal amount of variance in activation map similarity (City block/vertex task R^2 = 0.0024) compared with persistent individual differences (City block/vertex subject R^2 = 0.8649). In contrast, the difference between the "math" and "reward" condition in the Language task explained a greater amount of variance (City block/vertex task R^2 = 0.0632), with a comparable percentage of explained variance due to between-person differences (City block/vertex subject R^2 = 0.8632). Consistent with the total MDMR results, there was an increase in explained variance due to between-person differences and decrease due to task conditions when moving from lower to higher ROI resolutions. An additional observation of note is that areas of high between-person standard deviation (*SD*) had a consistent overlap with areas of high magnitude activation estimates across all task conditions (Figure 3). Thus, brain areas highly responsive to task conditions on average, across subjects, exhibit the greatest between-person variability in those responses compared with low-response areas. In addition, activation pattern similarity was greater across high *SD* vertices (top 20%) compared with low *SD* vertices (bottom 20%; Supporting Information Figure S2). As these high *SD* vertices overlapped with high average activation vertices, these findings indicate that activation pattern similarity was greater in task-response vertices, compared with nontask-responsive vertices.

3.3 | Clustering results

To further examine the type of experimental manipulations across task conditions that produce disparate or similar activation patterns across subjects, we used a graph-based clustering approach. We first computed a whole-brain activation pattern similarity matrix across all subjects' activation maps. The similarity matrix was constructed by computing the Euclidean similarity (inverse of distance) across all ROIs of the Schaefer 100 parcellation between all subjects' activation maps. We chose the Euclidean metric and Schaefer 100 ROI parcellation because this resolution and metric were most responsive to task-conditions (Figure 2). The objective function of the graph-clustering algorithm contains a resolution parameter ("gamma") that controls whether the resulting clusters are large ("coarse") or small ("fine-grained"), what we refer to as the "dimensionality" of the clustering. To choose a value for this parameter, we searched across values of the parameter that maximized the across-run clustering consistency (see Section 2; Supporting Information Figure S3). We chose two cluster solutions: A low-dimensional (coarse) and high-dimensional (fine-grained) cluster solution.

The low-dimensional cluster solution yielded three large clusters (containing 9,306 out of 9,984 activation maps), corresponding to a language/motor (C5), social/emotion (C2), and working-memory/gambling/emotion/relational task clusters (C3) (Figure 4). The largest cluster (C3; *N* = 4,835) contained a wide variety of task conditions. One prominent commonality among these task conditions was that they required active

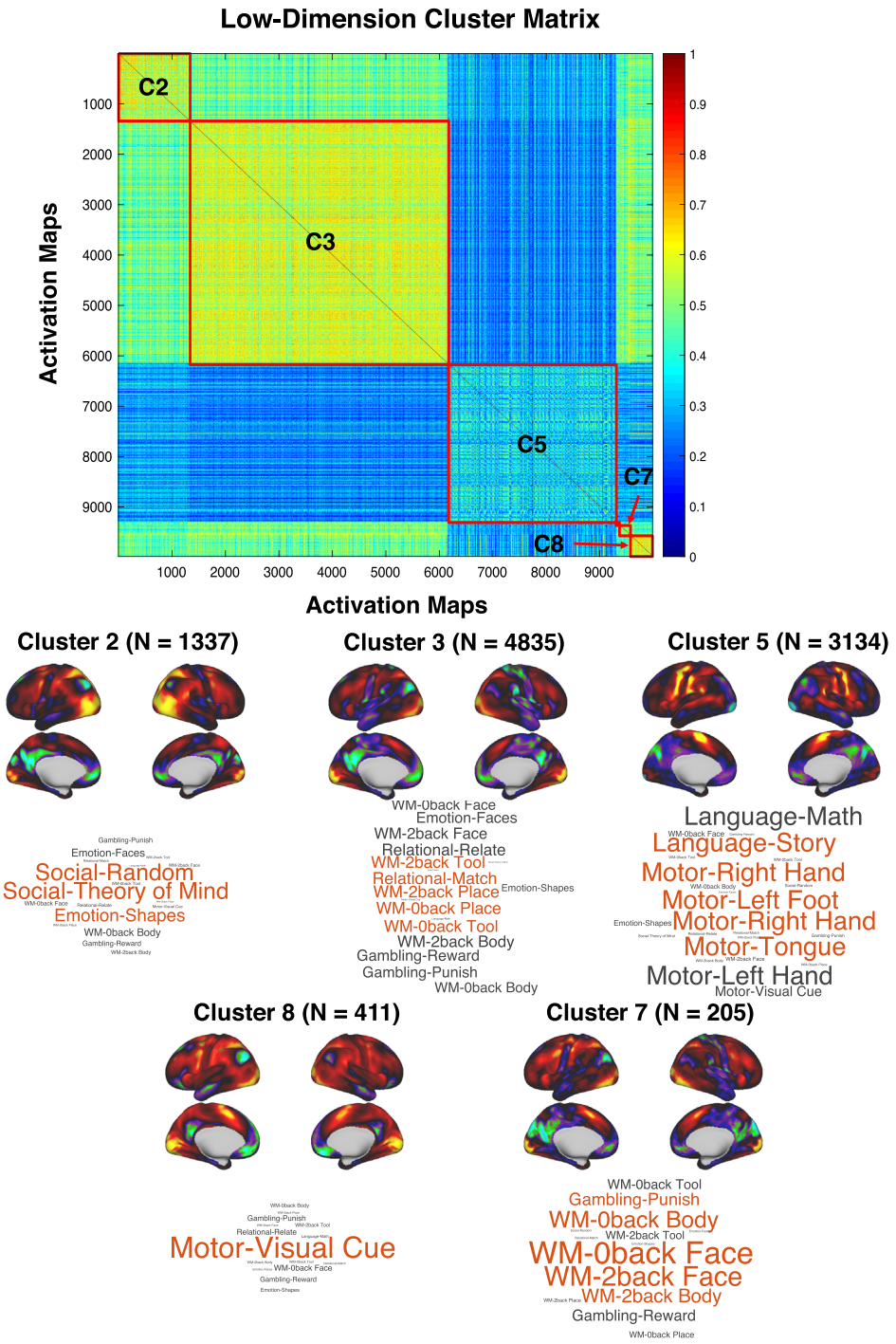

FIGURE 4 Low-dimensional clustering of whole-brain activation maps. Cluster-organized similarity matrix (left) and centroid activation maps/word clouds (right) for low-dimensional (gamma = 1.04) cluster solution. Values of the similarity matrix vary from 0 (cool colors) to 1 (warm colors), where 1 represents complete similarity between whole-brain activation maps, and 0 represents complete absence of similarity. Clusters of the similarity matrix are outlined with a red box and labeled with their corresponding cluster number (e.g., Cluster 2 = C2). Each cluster has an associated cluster centroid activation map and word cloud, representing the average activation pattern (computed across all vertices) and the number of task conditions that appear in that cluster by the size of its text, respectively. Beside each cluster label (e.g., Cluster 2) is the number of activation maps that appear in that cluster [Color figure can be viewed at wileyonlinelibrary.com]

attention to rapidly presented visual cues. This was not the case for the activation maps that belonged to the other two large clusters, C2 and C5. C2 primarily contained activation maps from the task conditions of the social task, which required passive viewing of visual stimuli. C5 primarily contained activation maps from the task conditions of the language and motor tasks, which involved responding to auditory stimuli and movements of various body parts to visual cues, respectively. Two smaller clusters, C7 and C8, were also present in the clustering solution. C7 (N = 205) primarily contained face and body stimuli conditions from the working memory task (both from the 0-back and 2-back conditions). C8 (N = 411) primarily contained the visual cue task condition activation maps from the motor task. While most activation maps belonging to a

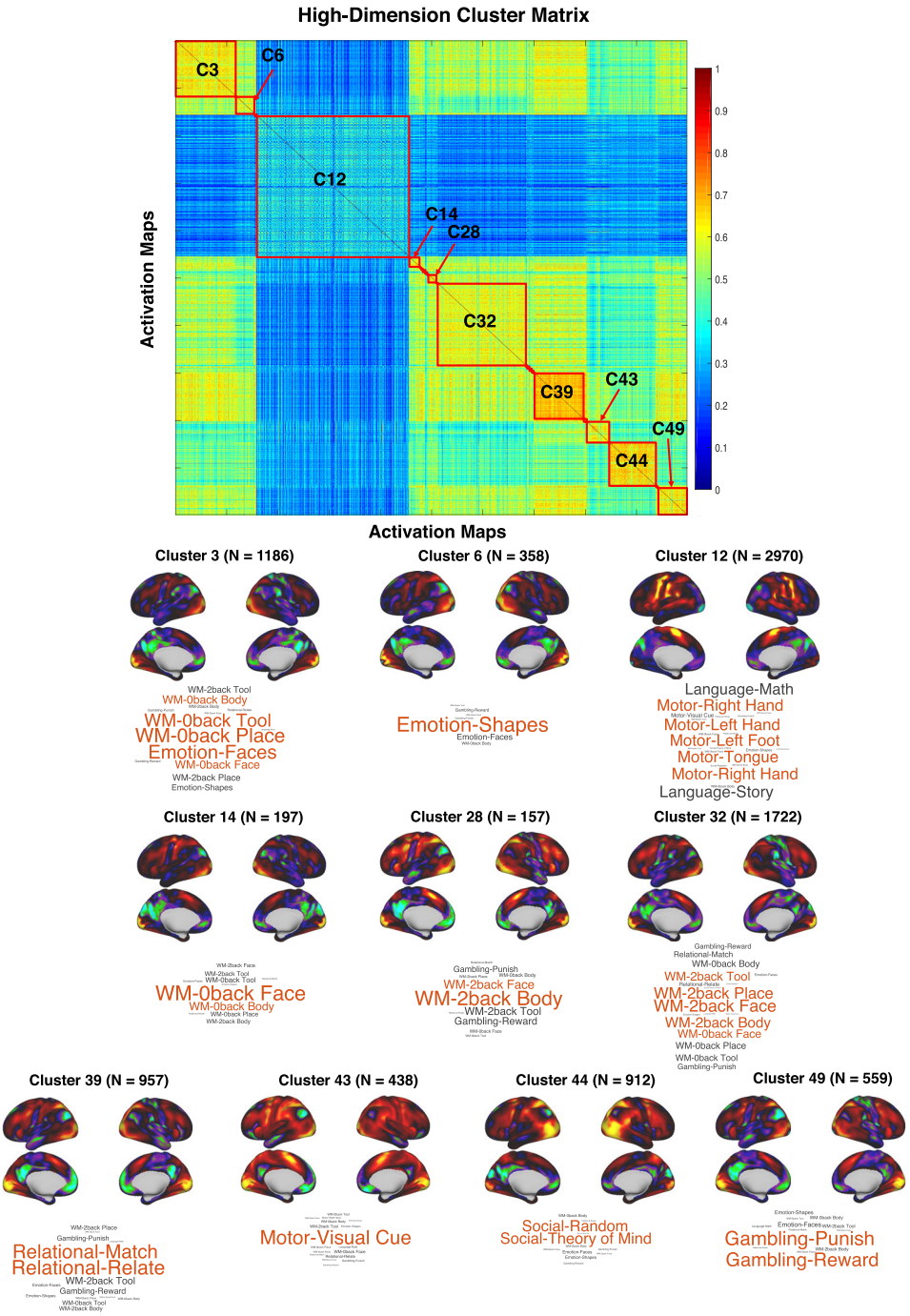

FIGURE 5 High-dimensional clustering of whole-brain activation maps. Cluster-organized similarity matrix (left) and centroid activation maps/word clouds (right) for high-dimensional (gamma = 1.13) cluster solution [Color figure can be viewed at wileyonlinelibrary.com]

single task-condition were classified into the same cluster, this was not the case for every task condition. For example, the activation maps for the "shapes" condition of the Emotion task was roughly split between C2 (N = 229) and C3 (N = 131). Notably, the social task activation maps that primarily constitute C2 were elicited by passive viewing of visual shapes. Thus, these observations suggest that some subject's activation maps look more similar to other task conditions (e.g., social task) than other subject's activation maps of the *same task condition*.

The high-dimensional cluster solution yielded a more "fine-grained" view of the relationships among the activation maps (Figure 5). Half of the clusters in this solution primarily contained activation maps from either a single task condition or task paradigm. C6 primarily contained activation maps from the Emotion task, C39 with the task conditions of the relational task, C43 with the visual cue condition of the motor task, C44 with the task conditions of the social task, and C49 with the task conditions of the gambling task. The task condition activation maps of the working-memory task were split between four clusters: C3 with primarily "0-back" conditions and the "face" condition of the Emotion task, C14 with "0-back" body and face stimuli conditions, C28 with "2-back" body and face stimuli conditions, and C32 with primarily "2-back"

conditions. Interestingly, the language/motor cluster from the low-dimensional cluster solution remained mostly intact in C12 of the high-dimensional cluster solution.

We also tested the degree to which the low- and high-dimensional clustering of whole-brain activation maps is driven by between-person differences, regardless of task conditions. We calculated the normalized mutual information (NMI; Meilă, 2007) between the cluster membership and subject membership of each activation map (varies from 0 to 1; 1 representing maximum similarity). The NMI between the cluster membership and subject membership indices was 0.0231 for the low-dimensional solution, and 0.0901 for the high-dimensional solution. In other words, the contribution of between-person differences to the low- and high-dimensional cluster solutions is minimal. However, the NMI values are nonzero, indicating that between-person differences did contribute to the cluster solution for some subjects.

4 | DISCUSSION

4.1 | Between-person and task-condition differences in BOLD activity

The primary goal of this study was to estimate the variability in BOLD activation maps explained by between-person and task-condition differences using a novel MDMR approach. In addition, we sought to determine the moderating influences on these estimates. Such influences include parcellation resolution, choice of distance metric, and task-paradigm coding. In agreement with Gratton et al. (2018), we find that task conditions explain greater variance between whole-brain activation pattern differences compared with persistent individual differences. This was the case for all parcellation "resolutions" considered. However, at the vertex-level (N = 59,412), we find that between-person differences explained a greater amount of variance than task conditions, for at least the City block distance metric, in agreement with Miller et al. (2009). More generally, we find that as the resolution at which whole-brain activation maps are compared increases, the variance explained by between-person differences increases more than that explained by task-condition differences decreases. This finding should not be surprising, given that there is much more variability in the fine-scale structure of the human cortex, as opposed to its large-scale arrangement. While comparing whole-brain activation patterns at lower ROI resolution reduces the dimensionality of the comparison, it also acts as a spatial smoothing operation, reducing potential small differences in the anatomical location of functional areas (Bijsterbosch et al., 2018; Mikl et al., 2008). Thus, increasing the parcellation resolution (e.g., 800 ROI parcellation or vertex-level) would reduce the extent of this implicit smoothing, thereby potentially increasing inter-subject variability of whole-brain activation patterns. Of note, spatial smoothing in the pre-processing of task-activation maps was minimal, 4 mm FWHM geodesic Gaussian smoothing. On the other hand, task condition differences in whole-brain activation patterns are most evident at the coarse ROI level (e.g., 100 ROI parcellation), suggesting that differences between task conditions are most likely to be reflected in large-scale spatial changes in task-evoked activity.

4.2 | Differences across levels of resolution

A corollary of this finding is that stable between-person differences in whole-brain activation patterns evoked by a task are largely due to small differences in the spatial extent of task-evoked activity that are more resolved at the vertex- or "fine-grained" ROI-level, as opposed to a "coarser" ROI parcellation. These small individual differences in the spatial extent in BOLD activation are not guaranteed to represent the spatial extent of task-responsive neural populations between subjects. At the resolution of a vertex or voxel, individual variability may be due to differences in vascular innervation or cross-subject alignment of neuroanatomical features, such as cortical folding patterns. In terms of vascular innervation, the measured spatial specificity of blood flow changes induced by neurovascular coupling is limited in gradient-echo (GE) BOLD fMRI due to venous drainage from the site of a task-responsive neural population. In fact, changes in venous blood flow can be detected as activation as far as 4 mm away from a task-activated neural population (Parkes et al., 2005; Turner, 2002), well above the 2 mm voxel resolution now commonly used in GE-BOLD fMRI (and the surface vertex-level used here). In addition, cross-subject alignment of anatomical features could still be an issue at a "high" resolution. Though a sophisticated multimodal surface normalization procedure (MSM-All) was used by the HCP for this dataset (Glasser et al., 2013), cross-subject alignment issues, however minimal, are still likely to be present (Guntupalli, Feilong, & Haxby, 2018). These factors make for a complicated interpretation of whole-brain activation pattern comparisons at a "fine-grained" resolution near to the vertex or voxel-level, which would not be present a coarser ROI parcellation level.

One central matter is what level of resolution is of greatest interest to task-fMRI researchers. It is a common practice to only interpret clusters of significantly active voxels/vertices with cluster-correction based thresholding techniques. In this case, larger brain regions are of interest, rather than individual vertices/voxels (Smith & Nichols, 2009). Furthermore, some researchers may restrict their analysis to a priori regions of interest from a data-driven parcellation (Gordon et al., 2017; Power et al., 2011) or previously reported brain coordinates. However, in some analyses of task fMRI data, interpretation of BOLD activity at the voxel/vertex level is a common practice. For example, multivariate pattern analysis (MVPA) commonly analyzes patterns of BOLD activity estimated at the voxel/vertex level. In analyses of the hemodynamic response using task-fMRI data, it is also quite common to analyze at the voxel/vertex level to distinguish different vascular components of brain tissue (e.g., large veins vs. capillaries). Thus, we reiterate the sentiment of Schaefer et al. (2017) and others that there is likely no optimal resolution for all task-fMRI analyses. The level of resolution, and thus the degree of between-person heterogeneity, will be dependent on the research question.

4.3 | Mathematical and empirical differences in distance metrics

This study also highlights the fact that similarity/distance metrics can perform differently in different contexts. For example, we find that whole-brain activation patterns are less different across task-conditions when the City block distance metric was used, as opposed to the

Euclidean distance. This was reversed for between-person differences: Whole-brain activation patterns are less different across subjects when the Euclidean distance was used, as opposed to the City block distance. The differences between the Euclidean and City block distances used here, as well as the Pearson correlation and cosine distance, can be explained in terms of their weighting of large distances. Properly normalized (i.e., *z*-scored beforehand to eliminate mean and scaling differences), City block, Euclidean, and Pearson Correlation/Cosine distance differ solely in terms of the weight given to the difference between two points when comparing two vectors. City block distance is the least sensitive to large differences, simply summing the absolute differences between each vertex/ROI between whole-brain activation patterns. The Euclidean distance sums the *square* of the difference between each vertex/ROI, followed by taking the square root of this sum. This squaring operation gives large differences between the activation estimates of a vertex/ROI differentially more weight compared to smaller differences. The correlation and cosine distance (equivalent if the mean is subtracted from each vertex/ROI) are equivalent (up to a constant factor) to the *z*-score normalized *squared* Euclidean distance: Simply summing the squared differences *without* taking the square root of this sum, which places even greater weight on larger differences. As illustrated above, these mathematical properties produce concrete empirical differences in the MDMR analyses above (Figure 2). For a concrete example, task-condition explains 46.68% of the variability in whole-brain activation pattern differences for the City block distance, 49.81% of the variability for the Euclidean distance, and 73.89% of the variability for the Pearson correlation/cosine distance. However, the differences between the distance metrics are likely more pronounced in our sample of task-activation maps. As can be observed from both the task-condition mean activation maps (Figure 3) and clustering results (Figure 5), many of the activation maps in this sample exhibit the same canonical task-positive/task-negative activation pattern. Differences between activation maps are mostly restricted to focal regions of this dominant task-positive/task-negative activation pattern. Thus, the City block distance would be more sensitive to the overall dominant task-positive/task-negative activation pattern and place less weight on these "outlier" regions. In contrast, the Euclidean and correlation/cosine distance would place greater emphasis on these "outlier" regions.

4.4 | Differences between task-conditions

A further issue in comparisons of between-person and task condition differences in BOLD activation patterns is the choice of task conditions. Task conditions with many different stimulus and response features would be expected to be more dissimilar in their evoked BOLD activation patterns than task conditions sharing largely the same features. In the case of a comparison between persistent individual differences and task conditions containing wildly different stimulus and response features, we would expect task conditions to explain a much greater amount of variance between whole-brain activation patterns than individual differences. This goes for differences between task conditions across task paradigms, as well as differences between task conditions within a task paradigm. For example, we observed very minimal differences between the task conditions of the gambling task. In fact, the difference in task conditions of the gambling task explained only 0.24% of the differences between whole-brain activation patterns at the vertex-level. This suggests that the different features between the conditions of the gambling task, mainly differing probability of gains versus losses, produce minimal observable changes in whole-brain activation patterns. In contrast, different features between the task conditions of the language task, auditory arithmetic calculations versus passive auditory listening to stories, explained 6.32% of the differences between whole-brain activation patterns at the vertex-level. These findings emphasize that the neural response estimated using BOLD fMRI is differentially responsive to experimental manipulations of the task-fMRI environment in ways that may not be expected by current cognitive theory. This further motivates a cognitive ontology project that attempts to identify those features of the task-fMRI environment that explain the greatest differences in whole-brain BOLD activation patterns (Anderson, 2015; Bolt et al., 2017; Lenartowicz et al., 2010; Poldrack & Yarkoni, 2016).

4.5 | Other factors contributing to differences in BOLD activation patterns

Several factors that could contribute to differential estimates of between-person and task condition variability were not explored in the main results of this manuscript:

4.5.1 | Thresholding

One such factor concerns the use of a *threshold* applied to the activation maps (as is conventional in much of task-fMRI) before computation of the distance between activation maps. For an initial insight into the contribution of this factor to between-person and task-condition differences, we applied a *z*-score threshold ($z > 2$) to each map of the 800-ROI resolution activation maps. We then applied an identical MDMR analysis to the analysis of the *unthresholded* maps in the main results. For thresholded maps, we found that the variability in BOLD activation maps explained by between-person and task condition differences decreased, as compared with the unthresholded maps. In other words, thresholding did not differentially affect estimates of between-person and task condition differences.

4.5.2 | Volume-versus-Surface Approach

Another factor is volume- versus surface-based analyses. We chose to use the cortical surface activation maps for our analysis, as surface-based registration approaches are known to provide superior alignment of cortical structure compared with volume-based approaches (Anticevic et al., 2008). Although we do not provide a direct comparison, this fact makes it likely that the MDMR analysis applied to cortical volume activation maps would result in higher estimates of between-person differences compared with the cortical surface activation maps used in the current study. An important omission in this study is subcortical structures, which have generally been neglected in most studies of individual variability of cortical activation and connectivity. To make our findings directly relevant to previous studies we also excluded subcortical structures, but note that these findings may not generalize to other areas outside of the cerebral cortex.

4.5.3 | Definition of ROI

Another factor is how ROIs are defined, and how "activation estimates" are computed from the defined ROIs. We chose to use the Schaefer et al. (2017) parcellation, due to the fact it provides multiple levels of resolutions (e.g., 100, 200, 400, and so forth). In addition, there are several potential routes for computing an activation estimate for each ROI in a parcellation: (a) The average of all vertices/voxels contained in the ROI, (b) weighted average of all vertices/voxels contained in the ROI, based on spatial uncertainty estimates, or (c) eigenvector/eigenvalue of vertices/voxels contained in the ROI. In this study, we chose the conventional averaging approach (a). However, approaches such as (b) and (c) are likely to reduce variability between-persons by accounting for potential spatial heterogeneity.

4.6 | Unsupervised clustering of activation maps

To identify those features in our sample of task conditions that produce disparate or similar activation patterns we used a graph-based clustering approach. Observations of both a low- and high-dimensional cluster solution yielded interesting findings. The cluster solutions revealed similarities in whole-brain activation patterns across task conditions and task paradigms. In the low-dimensional clustering solution, three large clusters were observed that contained primarily social/emotion (C2), language/motor (C5), and working-memory/gambling/relational/emotion (C3) task-condition activation maps. The task condition activation maps that belonged to the three clusters had quite distinct stimulus and response features. C2 activation maps primarily involved passive reception of visual stimuli. Of note, many of the "shape" condition activation maps of the emotion task also belonged to this cluster, which involved identifying whether simple line-drawn circles and ovals are the same or different. The ease of the task demands in this condition may be similar to passive reception of visual stimuli. C5 activation maps almost exclusively contained activation maps from the language and motor tasks, involving responses to presented arithmetic or story stimuli, and motor movements of hands, feet, or tongue regulated by a flashing visual fixation cross. The clustering results also revealed interesting observations regarding between-person differences. In both the low- and high-dimensional cluster solutions, some subject's BOLD activation maps were more similar to other task-conditions, than other subject's activation maps in the *same task condition*. For example, the activation maps for the "shapes" condition of the Emotion task was roughly split between two clusters in the low-dimensional cluster solution.

One notable observation from both cluster solutions is the high overall similarity in whole-brain centroid activation patterns between all clusters. This pattern is the classic "task-positive/task-negative" activation pattern that is consistently observed across a large variety of task paradigms (Bolt et al., 2017; Fedorenko, Duncan, & Kanwisher, 2013; Hugdahl, Raichle, Mitra, & Specht, 2015; Raichle et al., 2001). Minor differences in this overall pattern are what distinguish most centroid activation patterns of each cluster from each other. For example, C2 and C3 from the low-dimensional cluster solution are largely differentiated in terms of the differential higher activation in the lateral posterior cortex (Figure 5). These findings are consistent with a previous description of the nested structure of whole-brain BOLD activation patterns (Bolt et al., 2017), in which task-states are differentiated terms of permutations of a canonical task-positive/task-negative activation pattern.

5 | CONCLUSION

The results of this study suggest that the relative contribution of stable between-person differences versus task condition changes on task-evoked activity is difficult to determine. Our results demonstrate that the answer can depend on several additional factors: The parcellation "resolution", choice of distance metric, and coding of task conditions. With regards to parcellation resolution, variability in large spatial scale activity patterns is more associated with task condition differences than between-person differences, while variability in fine spatial scale activity patterns is more associated with between-person differences than task condition differences. Firm conclusions will also depend on other factors not examined here. For example, GLM beta maps used here as representative of "task-evoked" activity hardly exhaust the characterization of the brain's BOLD task response (Bolt, Nomi, Vij, Chang, & Uddin, 2018; Cole, Bassett, Power, Braver, & Petersen, 2014; Gonzalez-Castillo et al., 2012). In other words, the extent of between-person variability in task-evoked activity will depend on how one defines "task-evoked" activity. In addition, while the seven task paradigms provided by the HCP cover a broad range of behavioral domains, they miss task paradigms from other domains (action inhibition, introspection, and so forth) that may produce disparate results from the seven task paradigms studied here. We hope this study further clarifies the factors influencing between-person variability in task-evoked activity and encourages further study into the sources of individual differences in BOLD fMRI data.

ORCID

Taylor Bolt https://orcid.org/0000-0002-0533-3010

REFERENCES

Anderson, M. L. (2015). Mining the brain for a new taxonomy of the mind. *Philosophy Compass*, *10*, 68–77.

Anticevic, A., Dierker, D. L., Gillespie, S. K., Repovs, G., Csernansky, J. G., Van Essen, D. C., & Barch, D. M. (2008). Comparing surface-based and volume-based analyses of functional neuroimaging data in patients with schizophrenia. *NeuroImage*, *41*, 835–848.

Barch, D. M., Burgess, G. C., Harms, M. P., Petersen, S. E., Schlaggar, B. L., Corbetta, M., … WU-Minn HCP Consortium. (2013). Function in the human connectome: Task-fMRI and individual differences in behavior. *NeuroImage*, *80*, 169–189.

Bernstein, L. J., Beig, S., Siegenthaler, A. L., & Grady, C. L. (2002). The effect of encoding strategy on the neural correlates of memory for faces. *Neuropsychologia*, *40*, 86–98.

Berthold MR, Höppner F. 2016. On clustering time series using Euclidean distance and Pearson correlation. *ArXiv*1601.02213 Cs Stat.

Betzel, R. F., & Bassett, D. S. (2016). Multi-scale brain networks. *NeuroImage*, *160*, 73–83.

Bijsterbosch, J. D., Woolrich, M. W., Glasser, M. F., Robinson, E. C., Beckmann, C. F., Van Essen, D. C., … Smith, S. M. (2018). The relationship between spatial configuration and functional connectivity of brain regions. *eLife*, *7*, e32992.

Blondel, V. D., Guillaume, J.-L., Lambiotte, R., & Lefebvre, E. (2008). Fast unfolding of communities in large networks. *Journal of Statistical Mechanics: Theory and Experiment*, *2008*, P10008.

Bolt, T., Nomi, J. S., Vij, S. G., Chang, C., & Uddin, L. Q. (2018). Inter-subject phase synchronization for exploratory analysis of task-fMRI. *NeuroImage*, *176*, 477–488.

Bolt, T., Nomi, J. S., Yeo, B. T. T., & Uddin, L. Q. (2017). Data-driven extraction of a nested model of human brain function. *The Journal of Neuroscience*, *37*, 7263–7277.

Cole, M. W., Bassett, D. S., Power, J. D., Braver, T. S., & Petersen, S. E. (2014). Intrinsic and task-evoked network architectures of the human brain. *Neuron*, *83*, 238–251.

Delgado, M. R., Gillis, M. M., & Phelps, E. A. (2008). Regulating the expectation of reward via cognitive strategies. *Nature Neuroscience*, *11*, 880–881.

Eickhoff, S. B., Constable, R. T., & Yeo, B. T. T. (2018). Topographic organization of the cerebral cortex and brain cartography. *NeuroImage*, *170*, 332–347.

Fedorenko, E., Duncan, J., & Kanwisher, N. (2013). Broad domain generality in focal regions of frontal and parietal cortex. *Proceedings of the National Academy of Sciences of the United States of America*, *110*, 16616–16621.

Fink, G. R., Marshall, J. C., Weiss, P. H., Toni, I., & Zilles, K. (2002). Task instructions influence the cognitive strategies involved in line bisection judgements: Evidence from modulated neural mechanisms revealed by fMRI. *Neuropsychologia*, *40*, 119–130.

Finn, E. S., Shen, X., Scheinost, D., Rosenberg, M. D., Huang, J., Chun, M. M., … Constable, R. T. (2015). Functional connectome fingerprinting: Identifying individuals using patterns of brain connectivity. *Nature Neuroscience*, *18*, 1664–1671.

Fortunato, S., & Barthélemy, M. (2007). Resolution limit in community detection. *Proceedings of the National Academy of Sciences of the United States of America*, *104*, 36–41.

Geerligs, L., Rubinov, M., Cam-CAN, & Henson, R. N. (2015). State and trait components of functional connectivity: Individual differences vary with mental state. *The Journal of Neuroscience*, *35*, 13949–13961.

Glasser, M. F., Sotiropoulos, S. N., Wilson, J. A., Coalson, T. S., Fischl, B., Andersson, J. L., … WU-Minn HCP Consortium. (2013). The minimal preprocessing pipelines for the human connectome project. *NeuroImage*, *80*, 105–124.

Glover, G. H. (1999). Deconvolution of impulse response in event-related BOLD fMRI. *NeuroImage*, *9*, 416–429.

Gonzalez-Castillo, J., Saad, Z. S., Handwerker, D. A., Inati, S. J., Brenowitz, N., & Bandettini, P. A. (2012). Whole-brain, time-locked activation with simple tasks revealed using massive averaging and model-free analysis. *Proceedings of the National Academy of Sciences of the United States of America*, *109*, 5487–5492.

Gordon, E. M., Laumann, T. O., Gilmore, A. W., Newbold, D. J., Greene, D. J., Berg, J. J., … Dosenbach, N. U. F. (2017). Precision functional mapping of individual human brains. *Neuron*, *95*, 791–807.e7.

Gratton, C., Laumann, T. O., Nielsen, A. N., Greene, D. J., Gordon, E. M., Gilmore, A. W., … Petersen, S. E. (2018). Functional brain networks are dominated by stable group and individual factors, not cognitive or daily variation. *Neuron*, *98*, 439–452.e5.

Guntupalli, J. S., Feilong, M., & Haxby, J. V. (2018). A computational model of shared fine-scale structure in the human connectome. *PLoS Computational Biology*, *14*, e1006120.

Hugdahl, K., Raichle, M. E., Mitra, A., & Specht, K. (2015). On the existence of a generalized non-specific task-dependent network. *Frontiers in Human Neuroscience*, *9*, 430. https://doi.org/10.3389/fnhum.2015.00430.

Iaria, G., Petrides, M., Dagher, A., Pike, B., & Bohbot, V. D. (2003). Cognitive strategies dependent on the hippocampus and caudate nucleus in human navigation: Variability and change with practice. *The Journal of Neuroscience*, *23*, 5945–5952.

Lenartowicz, A., Kalar, D. J., Congdon, E., & Poldrack, R. A. (2010). Towards an ontology of cognitive control. *Topics in Cognitive Science*, *2*, 678–692.

Meilă, M. (2007). Comparing clusterings—An information based distance. *Journal of Multivariate Analysis*, *98*, 873–895.

Mikl, M., Marecek, R., Hlustík, P., Pavlicová, M., Drastich, A., Chlebus, P., … Krupa, P. (2008). Effects of spatial smoothing on fMRI group inferences. *Magnetic Resonance Imaging*, *26*, 490–503.

Miller, M. B., Donovan, C.-L., Bennett, C. M., Aminoff, E. M., & Mayer, R. E. (2012). Individual differences in cognitive style and strategy predict similarities in the patterns of brain activity between individuals. *NeuroImage, Neuroergonomics: The Human Brain in Action and at Work*, *59*, 83–93.

Miller, M. B., Donovan, C.-L., Van Horn, J. D., German, E., Sokol-Hessner, P., & Wolford, G. L. (2009). Unique and persistent individual patterns of brain activity across different memory retrieval tasks. *NeuroImage*, *48*, 625–635.

Miller, M. B., Van Horn, J. D., Wolford, G. L., Handy, T. C., Valsangkar-Smyth, M., Inati, S., … Gazzaniga, M. S. (2002). Extensive individual differences in brain activations associated with episodic retrieval are reliable over time. *Journal of Cognitive Neuroscience*, *14*, 1200–1214.

Parkes, L. M., Schwarzbach, J. V., Bouts, A. A., Deckers, R. H. R., Pullens, P., Kerskens, C. M., & Norris, D. G. (2005). Quantifying the spatial resolution of the gradient echo and spin echo BOLD response at 3 tesla. *Magnetic Resonance in Medicine*, *54*, 1465–1472.

Poldrack, R. A., & Yarkoni, T. (2016). From brain maps to cognitive ontologies: Informatics and the search for mental structure. *Annual Review of Psychology*, *67*, 587–612.

Power, J. D., Cohen, A. L., Nelson, S. M., Wig, G. S., Barnes, K. A., Church, J. A., … Petersen, S. E. (2011). Functional network organization of the human brain. *Neuron*, *72*, 665–678.

Raichle, M. E., MacLeod, A. M., Snyder, A. Z., Powers, W. J., Gusnard, D. A., & Shulman, G. L. (2001). A default mode of brain function. *Proceedings of the National Academy of Sciences of the United States of America*, *98*, 676–682.

Rosenberg, M. D., Finn, E. S., Scheinost, D., Constable, R. T., & Chun, M. M. (2017). Characterizing attention with predictive network models. *Trends in Cognitive Sciences*, *21*, 290–302.

Rubinov, M., & Sporns, O. (2010). Complex network measures of brain connectivity: Uses and interpretations. *NeuroImage*, *52*, 1059–1069.

Rubinov, M., & Sporns, O. (2011). Weight-conserving characterization of complex functional brain networks. *NeuroImage*, *56*, 2068–2079.

Schaefer, A., Kong, R., Gordon, E. M., Laumann, T. O., Zuo, X.-N., Holmes, A. J., … Yeo, B. T. T. (2017). Local-global parcellation of the human cerebral cortex from intrinsic functional connectivity MRI. *Cerebral Cortex New York*, *28*, 3095–3114.

Seghier, M. L., & Price, C. J. (2018). Interpreting and utilising intersubject variability in brain function. *Trends in Cognitive Sciences*, *22*, 517–530.

Shehzad, Z., Kelly, C., Reiss, P. T., Craddock, R. C., Emerson, J. W., McMahon, K., … Milham, M. P. (2014). An multivariate distance-based analytic framework for connectome-wide association studies. *NeuroImage*, *93*, 74–94.

Smith, S. M., & Nichols, T. E. (2009). Threshold-free cluster enhancement: Addressing problems of smoothing, threshold dependence and localisation in cluster inference. *NeuroImage*, *44*, 83–98.

Traud, A. L., Kelsic, E. D., Mucha, P. J., & Porter, M. A. (2011). Comparing community structure to characteristics in online collegiate social networks. *SIAM Review*, *53*, 526–543.

Turner, R. (2002). How much cortex can a vein drain? Downstream dilution of activation-related cerebral blood oxygenation changes. *NeuroImage*, *16*, 1062–1067.

Van Essen, D. C., Smith, S. M., Barch, D. M., Behrens, T. E. J., Yacoub, E., & Ugurbil, K. (2013). The WU-Minn human connectome project: An overview. *NeuroImage*, *80*, 62–79.

Woolrich, M. W., Ripley, B. D., Brady, M., & Smith, S. M. (2001). Temporal autocorrelation in univariate linear modeling of FMRI data. *NeuroImage*, *14*, 1370–1386.

Zapala, M. A., & Schork, N. J. (2006). Multivariate regression analysis of distance matrices for testing associations between gene expression patterns and related variables. *Proceedings of the National Academy of Sciences of the United States of America*, *103*, 19430–19435.

SUPPORTING INFORMATION

Additional supporting information may be found online in the Supporting Information section at the end of this article.

How to cite this article: Bolt T, Nomi JS, Bainter SA, Cole MW, Uddin LQ. The situation or the person? Individual and task-evoked differences in BOLD activity. *Hum Brain Mapp*. 2019;40:2943–2954. https://doi.org/10.1002/hbm.24570